American Journal of Engineering Research (AJER) 2016
American Journal of Engineering Research (AJER)
e-ISSN: 2320-0847 p-ISSN : 2320-0936
Volume-5, Issue-7, pp-79-84
www.ajer.org
Research Paper Open Access

Influence of High Strength Steel Microstructure on Fatigue Crack Growth Rate

Enefola S. Ameh[1], Basil O. Onyekpe[2]
[1](Department Of Mechanical Engineering, University Of Benin, Nigeria)
[2](Department Of Mechanical Engineering, University Of Benin, Nigeria)

ABSTRACT: *This study examines the effect of high strength steel microstructure morphology on fatigue crack growth rate (FCGR). To achieve this aim, three different heat treatment methods (normalizing, austempering quenching and tempering) were considered and all the steel specimens were initially heated to 950^{0}C austenization temperature for ninety minutes and then processed via the different heat treatment methods before viewing the resultant microstructures under light optical microscope (LOM). Fatigue crack growth rate tests were conducted on the resultant microstructures with compact tension specimens at room temperature as prescribed by American standard testing method E647. Results of FCGR tests showed normalized microstructure has the lowest FCGR (6.2698E-06), followed by quenched and tempered (7.9519E-06), as-received (8.15E-06) and austempered (9.6667E-06) microstructure considering a low stress intensity factor range. The trend of results showed insignificant effect of microstructure over the Paris regime growth indicating fatigue crack growth rate is not a reliable parameter for correlating rate of crack propagation to microstructure.*

Keywords: *FCGR, high strength steel, heat treatment, microstructure*

I. INTRODUCTION

High strength steels are increasingly in demand and have found wide application in offshore structures such as floating structures, pipelines, bridges, jacket structures and topsides owing to lower weight, lower manufacturing cost and ease of transportation but widely reported to be very susceptible to crack formation during welding, fabrication and in-service due to inherent high hardenability and influence of alloying elements despite its useful property [1]. Crack appearance could seriously reduce reliability of structures and components in-service and these crack and fatigue propagation are problems the society will continue to face as long as there are man-made-structures and components [2-3]. Most structural steels failure occurs because of crack presence that were either inherited during manufacturing, installation or in-service damage depending on the design and condition of service. Cracks under critical loads are preceded with crack growth, reduction in structural strength followed by final failure of the materials. The final failure occurs very fast and most times preceded with crack propagation, which grows steadily during normal service condition [4].

The most common approach in estimating fatigue crack growth rate is the use of Paris law. Fatigue integrity assessment of a critical component is usually performed by predicting the number of cycles required for crack to grow from an initial size to acceptable final size. Numerical integration of Paris equation predicts the number of cycles needed for the crack to grow from an initial length to final length [5]. The accuracy of using Paris formula to calculate fatigue crack growth rate of a cracked structure depends largely on the Paris coefficient, C and exponent m accuracy which are either experimentally obtained constant or from $\log da/dN$ versus $\log$ N plot. Paris equation is given as [6]:

$$da/dN = C(\Delta k)^m \quad (1)$$

or

$$\log da/dN = \log C + m \log \Delta k \quad (2)$$

Where, $\Delta k = k_{max} - k_{min} = S_{max}\sqrt{\pi a}\alpha - S_{min}\sqrt{\pi a}\alpha = \Delta S\sqrt{\pi a}\alpha$

C =intercept and m = slope of plot, $\propto$= geometry factor and can be obtained from each crack length, da = change in crack length, dN = change in number of cycle to failure. But in actuality, crack growth rate (da/dN)

depends on other factors other than Δk, which is the primary factor. Generally, formula for fatigue crack growth is given as:

$da/dN = f(\Delta k\ ,\ \mathrm{R},\ \ \mathrm{enviroment, frequency} \ldots)$ (3)

The Microstructure of high strength steel and it correlation to fatigue crack propagation are complex, diverse and can be changed by composition, heat treatment conditions and homogeneousness [7]. The microstructure influence on fatigue crack propagation or growth rate of steel still have contradictory literatures because of complexity with microstructural phases, constituents' formation mechanism and in addition to the fact that different microstructure offers different mechanical properties for the same chemical composition [8]. The present research work aim was to evaluate high strength steel microstructure morphology characterization and its influence on resistance to crack propagation. The practical relevance of investigating the effect of high strength microstructure on crack propagation rate includes improving the understanding of microstructure morphology effect on crack growth resistance which will greatly improve steel performance and extend design life of structure and components.

II. RESEARCH METHOD

2.1 Material Composition and Heat Treatments

Material used in the research work was 25mm thick plate of high strength steel and was procured from Masteel Company in UK. Chemical analysis of the steel sample was performed using optical emission spectroscopy method and the result revealed- 0.161% carbon, 0.296% silicon, 1.3% manganese, 0.011% phosphorus, 0.0006%sulphur, 0.0042% nitrogen, 0.03% cupper, 0.11% molybdenum, 0.051% nickel, 0.062% chromium, 0.002% vanadium, 0.026% niobium, 0.004% titanium, 0.0017% boron, 0.076% aluminum and the remaining percentage for iron agreed with the chemical composition supplied by the Company. All the test specimens were extracted from the steel plate and then machined to sizes slightly larger than the compact tension specimen's geometry prescribed by ASTM E647 standard and then machined to final dimensions after heat treatments. Three different heat treatment methods such as normalizing, austempering and quenching and tempering were considered and the test specimens were initially austenized to 950^0C and held for ninety minutes isothermal holding time. The sample for quenching and tempering was tempered to 550^0C in a furnace and held for ninety minutes while the austmpered sample was quenched in a liquid salt bath electric resistance furnace with fluidized potassium chloride (KCL) and Barium chloride ($BACl_2$) at 2:1 mole ratio and maintained at 350^0C for ninety minutes before being cooled in ambient temperature while the normalized specimen was cooled slowly in air from austenization temperature.

.

2.2 Fatigue Crack Growth Rate Tests

Fatigue tests were conducted according to ASTM E647 "Standard Test Method for Measurement of Fatigue Crack Growth Rate"[9]. All the specimens used for the tests were cut from the high strength steel in the rolling direction and machined to standard compact tension geometry and dimension indicated in Fig 1 and Table 1 respectively. Servo-hydraulic testing machine (Fig 2) equipped with a pair of clevises and a load capacity of 60KN was used for the tests. Fatigue pre-cracked specimens were setup between the clevises of the machine and securely fixed with pins prior to load application. All the fatigue tests were performed at constant amplitude loading which remained fixed throughout each specimen test. The applied loading range is between 10 to 35% yield strength of the material property. Fatigue cycle was conducted with sinusoidal waveform at a loading frequency of $10\mathrm{H_Z}$ and stress ratio R of 0.75. Direct current drop potential technique was employed during the tests to measure crack length a_i at certain number of cycles N_i for each specimen tested. The crack growth rate(da/dN) for each Δk was estimated using the mathematical expression [9]:

$da/dN = \frac{a_{i+1}+a_i}{N_{i+1}-N_i}$ (4)

An average crack size, $\bar{a} = 1/2\,(a_{i+1} + a_i)$ was used in the computation of Δk since da/dN computations are average rate over the increase of crack extension$(a_{i+1} + a_i)$. Crack extension was measured at interval of $\Delta a \leq 0.02W$ for $0.4 \leq a/W \leq 0.6$ so that da/dN data are rationally and equally distributed in relation to Δk. The range of stress intensity factor, Δk for CT specimen was calculated with the following equation:

$\Delta k = \frac{\Delta P}{B\sqrt{W}} f(a/W)$ (5)

Where the geometry factor $f(a/W)$ is defined as:

$$f(a/W) = \frac{2 + a/W}{(2 - a/W)^{3/2}}[0.886 + 4.64(a/W) - 13.32(a/W)^2 + 14.72(a/W)^3 - 5.6(a/W)^4]$$

Note: $\propto= (a/W)$ is the geometry factor and equation (5) is valid for $a/W \geq 0.2$

The number of cycles (N) for each crack length increment was calculated using Paris equation as follow:

$N = \int_{a_i}^{a_f} \frac{da}{C(\Delta k)^m}$ (6)

Table 1: CT Specimen dimensions

Quantity	Measured value (mm)
Specimen height (H)	1.2*W = 30.50
Specimen width (W)	25.40
Specimen thickness (B)	0.5*W = 12.70
Crack length (notch + pre-cracked)	0.45≤ a_o/W ≤0.55.
Notch Length (n)	0.25*W = 6.35
Pre-cracking length (L)	0.05B =0.64
Notch height (N)	0.1*W =2.54
Span length (S)	0.55*W = 13.97
Pin hole diameter (d)	0.25*W = 6.35
Total specimen length (T)	1.25*W =31.75

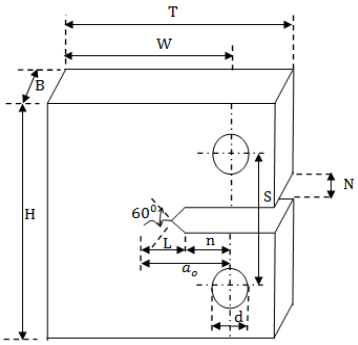

Figure 1: CT specimen geometry

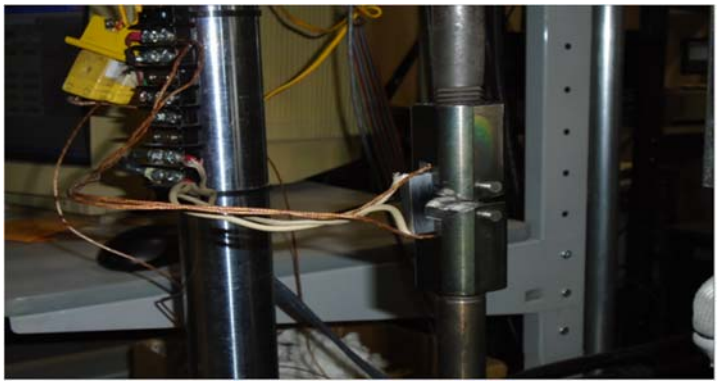

Figure 2: Servohydraulic Machine for FCGR Test

2.3 Characterization of Microstructure and Fracture Surface

The as-received and heat treated samples were ground with 120, 220, 600 and 1200 silicon carbide papers in decreasing coarseness of grit and then polished with 6 microns and 1 micron diamond paste respectively. Each polished sample was viewed under a light optical microscope shortly after dipping the surface into 2% nital (2% nitric acid and 95% ethanol) and dried. Facture surfaces of the FCGR of all the tested specimens were carried out to reveal crack propagation mode and mechanism and this was achieved by exposing half of the broken fractured surfaces of each sample to scanning electron microscope SEM at an accelerated voltage of 30KV and thereafter captured the fractographs.

III. RESULT AND DISCUSSIONS

3.1 Influence of Microstructure on FCGR

The resulting microstructure for the as-received steel and the different heat treated methods are shown in Fig 3. The graphs in Fig 4 showed da/dN versus Δk plot of the different steel microstructures to closely view and understand the influence of different microstructures on fatigue crack growth rate. It was noticed the fatigue crack growth rate for the different samples exhibited very similar characteristics indicating da/dN was not relatively sensitive to microstructure. The observation was in agreement with [10] that crack growth rate has low

strong influence on microstructure as a consequence of fatigue crack propagation being controlled by cyclic flow properties rather than monotonic tensile properties. However, Fig 4 showed microstructure of normalized steel has the lowest fatigue crack growth rate(6.2698E-06) at a lower stress intensity factor range, followed by quenched and tempered(7.9519E-06), as-received(8.15E-06) and austempered (9.6667E-06) microstructure. Normalized microstructure fatigue crack growth was found to decrease by a factor of 1.5 compared to austempered structure. The obvious significant difference can be explained by microstructure composition of normalized sample which consisted predominantly ferrite and pearlite phases in the structure and attributed to deflection from elongated ferrite grains.

FCGR of austempered macrostructure was found to increase in high Δk range by a factor of 1.2, 1.5 and 1.1 compared to the as-received, normalized and quenched and tempered microstructure respectively. The significant increase was probably largely due to the presence of microstructure of feathery appearance of upper bainite structure consisting short plate ferrite called sheaves and coarse ferrite and pearlite. Crack had readily propagated through sheave of bainite plate as a result of identical crystallographic orientation once the critical size microcrack was formed. Austempered microstructure revealed short bainite sheaves indicating crack deflection was low and consequently decreased resistance to crack growth. The as-received sample exhibited elongated fine grain structure resulting probably from the appreciable amount of cold working employed in the manufacturing process. Comparing the austempered sample with as-received, austempered microstructure exhibited abnormally coarsed grains which could be attributed to long isothermal holding time during austenization. The abnormal coarse grains subsequently become initiation site for cracks when subjected to external fatigue loads.

Crack growth rate of the quenched and tempered microstructure sample was found to be slightly less than the austempered microstructure sample and increased by a factor of 1.1 compared to the as-received. The difference can be explained by composition of the microstructure resulting from the tempering process. The long tempering broke down martensite structure to ferrite and brittle phase cementite (Fe_3C) to critical size value to favour crack propagation. Large grain boundary which means fewer grain boundaries promote crack nucleation and decrease resistance to crack growth under high stress. Crack growth rate largely depend on grain boundaries as much as the type of phases present. Fine grained structure is widely reported to give better resistance to crack growth rate due to higher grain boundary area per unit volume and the grain boundary acts as barrier to crack propagation [11].

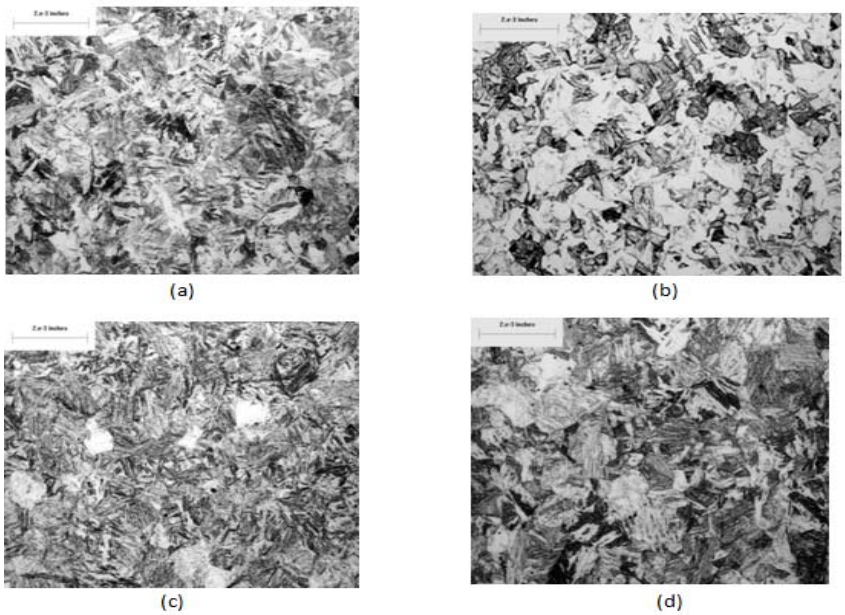

Figure 3: Microstructure (LOM X 1050) – **a)** As-received consist of martensite with traces of bainite, **b)** Normalized consist of ferrite/pearlite, **c)** Austempered consist of predominate lower bainite with traces of upper bainite sheaves, & **d)** Quenched and Tempered consist of blocks of martensite with traces of bainite.

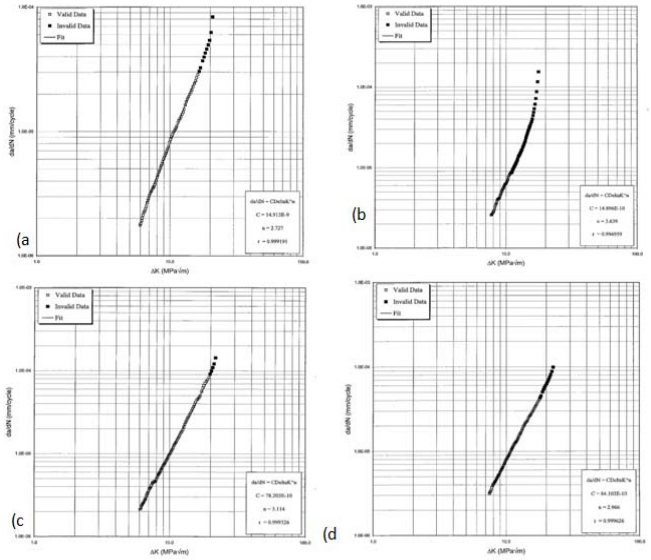

Figure 4: Plot of da/dN vs. delta k – **a)** As-received, **b)** Normalized, **c)** Austempered, & **d)** Quenched and Tempered

3.2 Fractographic Analyses

Fracture surface zones (Fig 5) taken from the middle of specimens that had undergone fatigue crack propagation indicated small quasi-cleavage facets with microvoids and coalescence distributed around it. Several and large cleavage facets associated with low crack propagation resistance increased with increasing crack propagation resistance. But Fig 5(a) and 5(b) distinctly showed several ridges (striations) perpendicular to the direction of crack propagation and Fig 5 (c) specifically showed several uniformly distributed tiny microvoids. The presence of coalescence of ridges and voids are attributed to repeated loads with subsequent cycles and accumulated damages and resistance to crack propagation. Physical observation of samples surfaces revealed fractured surface of normalized microstructure appeared most fairly uniform compared to the rest samples. The uniformity appearance of the cleavage facets, thus resulted in fine surface, and the finer and smaller facets, the more difficult crack propagation as the crack must change direction more often to propagate. Fracture surface morphologies of Fig 5 (a) and 5 (b) showed fairly rough surfaces with shallow dimples indicating stable crack growth phase with low fatigue crack growth rate compared to austempered and quenched and tempered microstructure. But Fig 5 (c) revealed very shallow and tiny dimples while Fig 5 (d) showed most coarse facet size. The FCGR fractured surface analysis agreed with the fatigue test results that indicated normalized microstructure had the lowest FCGR, followed by the as-received. But the fracture surface analyses of Fig 5 (c) and Fig 5 (d) suggested FCGR of austempered microstructure was lower than quenched and tempered microstructure contrary to FCGR test results since more coarse cleavage facets was expected to yield a lower cleavage crack growth resistance.

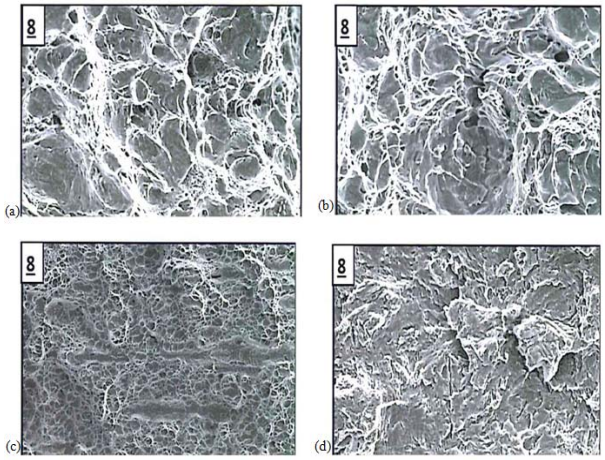

Figure 5: Fatigue crack growth fractured surface from specimen middle zone – **a)** As-received, **b)** Normalized, **c)** Austempered, & **d)** Quenched and Tempered

IV. CONCLUSION

Normalized microstructure has the lowest FCGR (6.2698E-06), followed by quenched and tempered (7.9519E-06), as-received (8.15E-06) and austempered (9.6667E-06) microstructure. Fatigue crack growth rate showed very low and insignificant sensitivity to microstructure morphology implying low reliability in predicting fatigue life of a structure. The study suggested soft ferrite matrix, carbide particles and dispersed cementite grains in ferrite are critical micro structural constituents that could possibly influence fatigue crack growth rate. The fractography of the fatigued surfaces showed cleared distinction of fracture morphology and provided significant information of failure modes.

REFERENCES

[1]. J.E. Ramirez, Characterization of high strength steel weld metals: chemical composition, microstructure, and non- metallic inclusions, Welding Journal, vol.87, 75-S.

[2]. G. Vukelic and J. Brinc, J-integral as possible criterion in material fracture toughness assessment, Engineering Review, issue 2, 2011, 91 – 96.

[3]. A. Gopichand, Y. Srinivas and A.V.N.L. Sharma, Computation of stress intensity factor of brass plate with edge crack using J-integral technique, International Journal of Research in Engineering and Technology, vol01, 2012, 2319 – 1163.

[4]. J. Veeranjaneyulu and H. R. Rao, Simulation of the crack propagation using fracture mechanic techniques in aero structures, International Journal of Engineering Research and Application, vol2, 2012, 1168-1173.

[5]. S.M. Beden, S. Abdullah and A.K. Ariffin, Review of fatigue crack propagation model for metallic components, European Journals of Scientific Research, vol. 28, 2009, 364-397.

[6]. Z. Zheng, B.E. Powell, J. Byrne, and W. Hussey, The characterization of fatigue crack growth behaviour by constant Δk control testing, Journal of Fatigue Fracture of Engineering and Material Structure, vol. 22, 1999, 383-392.

[7]. L.W. Ma, X. Wu and X. Kenong, Microstructure and property of medium carbon steel processed by equal channel angular pressing, Material forum Vol. 32, 2008, Pub. Institute of materials engineering Australasia ltd.

[8]. S. Al-rubaiey, E. Anon and M.M. Hanoon, The influence of microstructure on the corrosion rate of carbon steel, Engineering and Technological Journal, vol.31, 2013, part (A) No 10.

[9]. ASTM E1820, Standard test method for measurement of fracture toughness (ASTM International USA, 2010)

[10]. T.L. Anderson, Fracture mechanics - fundamentals and application (Third edition, Pub. CRC press, 2005).

[11]. G.E. Dieter, Mechanical metallurgy (Pub. Mc Graw-Hill, Singapore, Pp 346 – 369, 1988).